

Sloppy model analysis unambiguously identifies bifurcation parameters of all common types of bifurcations

Christian N. K. Anderson* and Mark K. Transtrum†

Department of Physics and Astronomy

Brigham Young University

Provo, UT 84604.

(Dated: January 21, 2022)

Bifurcation phenomena are common in multi-dimensional multi-parameter dynamical systems. Normal form theory suggests that the bifurcations themselves are driven by relatively few parameters; however, these are often nonlinear combinations of the bare parameters in which the equations are expressed. Discovering reparameterizations to transform such complex original equations into normal-form is often very difficult, and the reparameterization may not even exist in a closed-form. Recent advancements have tied both information geometry and bifurcations to the Renormalization Group. Here, we show that sloppy model analysis (a method of information geometry) can be used directly on bifurcations of increasing time scales to rapidly characterize the system's topological inhomogeneities, whether the system is in normal form or not. We anticipate that this novel analytical method, which we call time-widening information geometry (TWIG), will be useful in applied network analysis.

Keywords: bifurcation, normal form, sloppy modeling, information geometry, Fisher Information matrix

CONTENTS

I. Introduction	1
II. Background and Problem Formulation	2
A. Bifurcations	2
B. Information Geometry	3
III. Normal-form Bifurcations	5
IV. Bifurcations in Non-normal Forms	7
A. A biophysical example	8
V. Conclusion	9
A. FIM of Saddle-Node Bifurcations	9
1. Partial derivative of r	9
2. Partial derivative of α_1	10
3. Partial derivatives of higher-order α 's	10
B. FIM of Transcritical Bifurcations	10
1. Partial derivative of r	11
2. Partial derivative of α_1	11
3. Partial derivative of higher-order α 's	11
C. FIM of Pitchfork Bifurcations	11
1. Partial derivative of r	12
2. Partial derivative of α 's	12
D. FIM of Hopf Bifurcations	12
References	12

I. INTRODUCTION

This paper provides a method for extracting bifurcation parameters from a set of dynamic equations by combining information geometry and bifurcation theory. Both are useful for modeling multi-parameter systems and systems with multiple regimes of behavior respectively, but together they have the potential to provide methods for data-driven analysis of a wide array of natural phenomena. By creating an explicit connection between the information in the signal (model output) and the model parameters, we identify the combinations of parameters responsible for topological change in the dynamics, the co-dimension of the bifurcation, and the time-scale necessary to resolve this information. The information gives the directions normal to the separatrix, which divides behavioral regimes of the system.

Traditionally, when confronted with a high-dimensional, multi-parameter system of dynamic equations, bifurcation analysis proceeds by attempting to simplify the system to a manageable size. Center Manifold Reduction exploits the Hartman-Grobman theorem[1] to create a lower-dimensional linear map in the region of a critical point that is locally-accurate and is a rapid way to determine the system stability. Shoshitaivishili extended this method to non-hyperbolic equilibria, creating a container for critical modes to straighten out non-linear terms and, ideally, drop some of them[2]. Such methods have been used to describe phenomena as diverse as neural network optimization and foraging decisions in monkeys[3, 4].

A related approach is the method of Poincaré-Birkhoff normal forms. It uses appropriately centered manifolds to analyze which nonlinear terms are essential and must remain even under optimal coordinate transformations. Such transformations are useful, because the reduced

* bifurcate@byu.edu

† mktranstrum@byu.edu

normal-form equations typically have greater symmetry than the initial problem, a property that can be exploited by many analytical tools. Though powerful, “in practice lengthy calculations may be necessary to extract the relevant normal-form coefficients from the initial equations.”[2] Even if such coefficients can be found, neither their interrelationship nor their relative sensitivities are always apparent. It is often the case that some parameters differ by many orders of magnitude in their effect on long-term dynamics, and a method that doesn’t distinguish among them is sub-optimal for most applications.

The method of Luyupanov exponents is an admirably general tool for analyzing the global stability of a system. Unfortunately, it provides little information about which specific parameter combinations lead to system (in)stability. For the purposes of bifurcation analysis, it is therefore sometimes paired with sensitivity analyses based on Sobol’s global sensitivity metrics[5]. These measures, along with useful extensions such as FAST (Fourier amplitude sensitivity test) and Importance Measures[6–8], are able to determine exactly how much of a model’s variability is due to each of its parameters. While this often works in practice, there are two potential pitfalls in this approach. First, it assumes that the parameters responsible for variability are also responsible for instability, which is not always the case. Second, if the bifurcation is caused by combinations of many parameters (as frequently happens), then variability will often be high across all these parameters even though the bifurcation itself has a low codimension. In other words, a low-dimensional bifurcation surface generally cuts diagonally across parameter space unless appropriately reparameterized. Once such a transformation is applied and the system is reduced to a normal form (see Sec III), then the codimension should be apparent, but finding that reparameterization is still likely to be cumbersome, if not impossible in closed-form. Just one such transformation can require several papers, as in the case of high-dimensional diffusion-activated processes from Kramers, through Langer, and finally to one dimension, derived using iterations of singular value decomposition by Berezhkovskii[9].

A third, independent line of analysis comes from Renormalization Group (RG) theory. Feigenbaum[10] was the first to note universalities in bifurcations of the discrete period-doubling type, a result extended by himself and others until it included all major bifurcation types[11–15]. Working from the other direction, scientists investigating phenomena known to belong to the RG universality class (e.g., many behaviors of quantum chromodynamics) have discovered bifurcations, and used the tools of one to analyze the other[16]. Given the ubiquity of bifurcations in nature, it should not come as a surprise that they are found in a class wide enough to be called “universal”. A remarkable study found deep equivalence between RG transformations and Normal Form theory, showing that the difficult transformation of an ODE sys-

tem into a normal form could often be accomplished to at least second order by applying three RG transforms[17].

The Renormalization Group has been connected to methods of information geometry[18–22]. A recent theoretical paper[23] suggested that as coarse-graining of RG models proceeds, the flow causes information of “relevant” parameter combinations to be maintained while “irrelevant” parameters become indistinguishable from simpler models. We will demonstrate similar notions of “relevant” and “irrelevant” parameters near a bifurcation using the formalism of information geometry. This paper closes that loop, showing how information geometry applies directly to bifurcation analysis without passing through the “middleman” of renormalization group. The usefulness of such an analysis, which we call Time Widening Information Geometry (TWIG), also circumvents the need for the other types of analyses described above.

This paper is organized as follows: In Section 2, we provide background information on bifurcations and information geometry generally, and specifically how we conceptualize them for the purposes of applying the latter to the analysis of the former. In Section 3, we show how an IG analysis of the normal form bifurcations rapidly provides insight into the structure of bifurcations simple enough to be understood by other methods. Section 4 shows how this analysis extends to more difficult bifurcations, the implications of which are summarized in Section 5.

II. BACKGROUND AND PROBLEM FORMULATION

A. Bifurcations

Bifurcations frequently arise in the analysis of dynamical systems, where one typically characterizes the flow field with special attention to any fixed points or stable oscillations[24]. Consider a generalized system of n coupled dynamic equations, where each equation is of the form $\dot{\mathbf{y}} = f(\mathbf{y}; \theta)$, where θ is a vector of m parameters. Small changes to any of the θ_i values typically result in correspondingly small changes to the n -dimensional vector field, such as small changes to the position of a fixed point or radius of a limit cycle. Such deformations are topologically equivalent (meaning the number and properties of the attractors / repellers in the field do not change) and homeomorphic (continuous with a continuous inverse). However, there may be critical parameter values where a small change causes new fixed points to emerge from old ones, or two fixed points to approach and be mutually annihilated, or limit cycles to be broken. Since a common form of nonhomeomorphic transformation is the emergence of two fixed points from one, the phenomenon is generically called bifurcation, though any change in the number of nodes or cycles is theoretically possible.

Several types of simple bifurcations have been identified and reduced to their simplest possible mathematical expression. These are the so-called “normal forms” and are enumerated in the section below. These forms are convenient starting points for analysis, since they have clearly defined rate parameters that are unambiguously responsible for causing topological inhomogeneities. However, even elegant mathematical descriptions of real-world dynamical systems rarely conform exactly to one of the normal forms.

Bifurcation parameters for physical models often do not align with the bare parameters. In the classic boiling liquid, the bifurcation parameter is some combination of temperature, pressure, salinity, and others. In general, a reparameterization to a single, unambiguous bifurcation parameter may be possible in principle, but often requires either substantial additional physical insight, or mathematical sophistication, or both. Some researchers have even recommended building an analogous physical circuit as the fastest method to detect the bifurcation[25]. Complex models can have hundreds of coupled dynamical equations with thousands of parameters (e.g., models of sophisticated mobile phone circuit boards[26], or complex protein networks[27]). How can we determine which parameter (or more likely, combination of parameters) is responsible for the bifurcation in such cases?

B. Information Geometry

The fundamental object of information geometry is the Fisher Information Matrix (FIM or \mathcal{I}), which quantifies the information that the observations \mathbf{y} contain about the parameters θ of a dynamical system. Here we introduce the FIM for dynamical systems.

Consider a system of ordinary differential equations where the parameters are tuned to be exactly at their critical values, i.e., the system is at (one of) its bifurcation point(s). The system is allowed to evolve, and the trajectory of one of its equations y_j is sampled at several time points $y_j(t_i)$, where $t_i = t_0 + \frac{i}{n}t_{max}$. To help visualize this process, let us imagine a one-dimensional system

$$y(t) = \theta_1 + e^{-\theta_2 t} + e^{\theta_3 t} \quad (1)$$

sampled at $t = \{1, 2, 3\}$ to create a vector of three observations $\mathbf{y} = \{y(t_1), y(t_2), y(t_3)\}$ which we plot in \mathbb{R}^3 data space. If $\theta_3 > 0$, then there is no equilibrium; if $\theta_3 = 0$ and $\theta_2 > 0$ then the equilibrium is at $\theta_1 + 1$ or $\theta_1 + 2$ if $\theta_2 = 0$. As the parameters of θ change, the position of \mathbf{y} will also change, but except for extreme values of θ_i , it cannot reach all possible values in \mathbb{R}^3 . The space filled by all possible values of \mathbf{y} for a range of values in is the model manifold. Such a manifold is drawn in Fig. 1A.

The Fisher Information is defined in probabilistic terms as the expected Hessian matrix of the log-

likelihood:

$$\mathcal{I} = -E \left[\frac{\partial^2}{\partial \theta^2} \log \mathcal{L}(d|Y, \theta) \right] \quad (2)$$

For deterministic systems, such as we consider here, it is common to assume that the measurements are obscured by additive Gaussian noise, which defines a probability distribution to which Eq. 2 can be applied[28]. The resulting FIM is sometimes called the sensitivity Fisher Information Matrix or sFIM[29]. In this case, \mathcal{I} can be expressed in terms of the first derivatives only. In terms of the the Jacobian matrix $J_{k,j} = \frac{\partial y_k}{\partial \theta_j}$, it is given by

$$\begin{aligned} \mathcal{I} &= J^T J \\ \mathcal{I}_{i,j} &= \sum_{k=1}^m \frac{\partial y_k}{\partial \theta_i} \frac{\partial y_k}{\partial \theta_j}. \end{aligned} \quad (3)$$

The entries of the FIM indicate the sensitivity of the model’s trajectory to changes in each pair of parameters. A high score indicates that a parameter pair has a strong influence on model dynamics, while a small score indicates a “sloppy” direction (parameter values can change a great deal without much changing \mathbf{y}). The curvature of the likelihood function converts distances in parameter space to distances on the manifold in data space, making the FIM a Riemannian metric tensor.

Of course, there is no guarantee that the curvature of the likelihood surface will align with the bare parameters, rather, the ideal characterization of the model’s sloppiness aligns with the eigenvectors of \mathcal{I} . The above formula again comes to our aid, since, for the singular value decomposition of $J = U\Sigma V^T$, it follows that

$$\mathcal{I} = V\Sigma^2 V^T \quad (4)$$

This implies that the right singular values of the Jacobian V are also the eigenvectors of the FIM.

To summarize, using only partial first derivatives to create J and simply applying Eq. 3 to obtain \mathcal{I} , we are able to see the relative effects of 2-parameter combinations on overall dynamics. The eigenvalues of \mathcal{I} , which according to Eq. 4 are $\lambda_i = \Sigma_{ii}^2$ from the singular value decomposition of J , will therefore correspond to the relative sensitivity of the model to changes in each eigendirection, which eq. 4 also tells us are the columns of V . We are thus able to “orient” \mathcal{I} optimally in order to compare each eigendirection, whether they involve all the bare parameters or just one.

Returning to our simple example, imagine that we zoom-out our sampling by changing t_{max} from 3 to 6, so \mathbf{y} is now being sampled at $t = \{2, 4, 6\}$. This procedure will stretch the manifold in some eigendirections, and shrink it in others. This will be measured by an increase or decrease in the eigenvalues λ of \mathcal{I} , respectively. If the manifold shrinks in one eigendirection (or, equivalently, the corresponding eigenvalue decreases) with increasing t_{max} , this indicates that this combination of parameters is less important to the long-term dynamics,

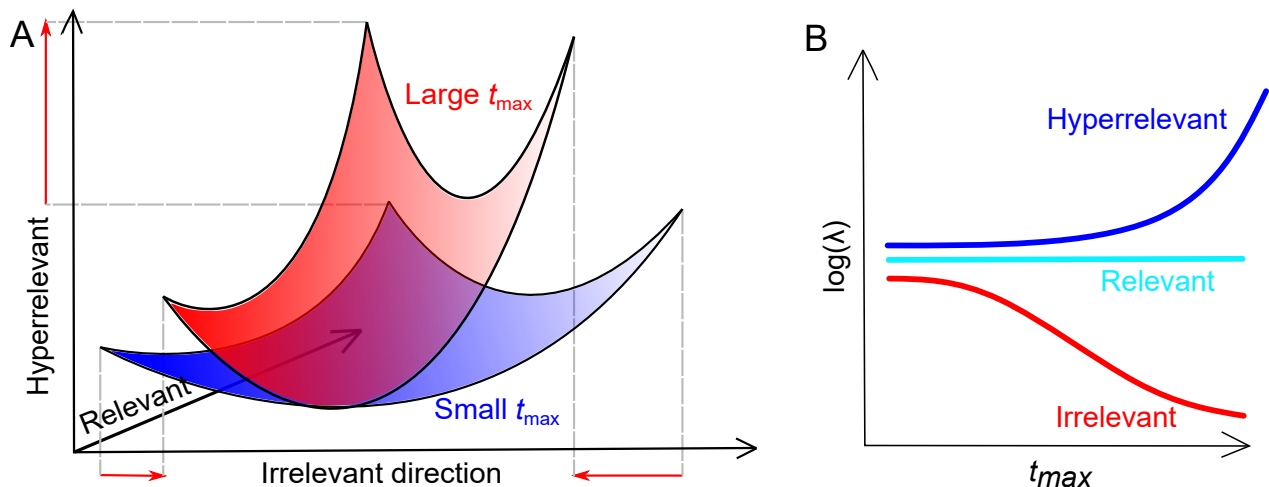


FIG. 1. (A) The model manifold in data space represents all values that can be reached. The axes represent directions that are distorted in characteristic ways as t_{max} increases. They can be contracted (irrelevant), expanded (hyperrelevant) or unchanged (relevant). (B) Relevance can be quantified by observing the eigenvalues of the Fisher Information Matrix as t_{max} is increased. Eigenvalues that do not change at longer time scales retain their relevance, while those that increase or decrease become either more or less relevant.

and the eigendirection is called “irrelevant”. If no such decrease occurs, we call this a “relevant” direction, and if it actually stretches / increases, this is evidence it is a “hyperrelevant” eigendirection (Fig. 1B). Returning to the example in equation 1, θ_3 will be hyperrelevant since changes will destroy the equilibrium, θ_2 will be irrelevant since the exact rate of the decay matters less as time scales become very large, and θ_1 will be relevant since its value changes the location but not the stability properties of the equilibrium.

This procedure is similar to coarse-graining under RG flow described in referece [23], and used to generate their Fig. 1. In our case, however, because we are coarsening the sampling rate, the total observation time increases and includes new information, i.e., observations at later times. As such, it is not a true coarse-graining, and introduces the possibility of hyperrelevant directions, i.e., directions that become increasingly important. We will see that hyperrelevant directions are associated with stability or instability of the equilibrium.

Such an analysis reveals two other features of the data. First, there can be parameters (or combination of parameters) that move the location of a fixed point without causing a bifurcation. Such parameter combinations appear as “relevant” eigendirections, as the new equilibrium appears in long-time observations. These parameters need to be removed in order to correctly identify the co-dimension of the bifurcation. We do this by solving for the location of the fixed point with a numeric RootFind algorithm and subtracting it from the trajectory at every point. This effectively translates the fixed point to the origin and is analogous to the recentering step of Center Manifold Analysis. For limit cycle trajectories we subtract off the (unstable) fixed point that must exist within

the cycle by the Poincaré-Bendixson theorem[30].

The second feature arises in such oscillating systems. Parameters that change the phase or frequency of oscillation without destroying the equilibrium itself appear as hyperrelevant as the accumulating phase differences becomes increasingly important at late times. Previous research has shown that such systems frequently cause problems in an Information Geometry framework by introducing “ripples” into the likelihood surface of Eq 2. The solution is to perform a coordinate transformation so the period itself becomes a parameter. In one formulation of the FIM, this causes the manifold to “unwind”, creating a smooth likelihood surface[31], or eliminating a misleading eigendirection in the context of this paper.

Four important pieces of information come from this Time Widening Information Geometry (TWIG) analysis. First, the number of hyperrelevant and relevant directions corresponds to the co-dimension of the bifurcation system. Second, the square of each element of the eigenvector matrix V_{ij} indicates the participation factor of each bare parameter θ_i in eigenvector j . This last fact follows because the participation factor $p_{ij} \equiv U_i^j V_i^j = V_{ij}^2$ combining the definition of a participation factor[32, 33] with equation 4 above. Third, the eigendirections themselves will change as t_{max} increases and parameters that influence the short-term dynamics lose their salience at long time scales. If initial conditions are included as parameters, their loss of relevance is a strong indicator that the system has been simulated “long enough” to capture equilibrium behavior. This is not a trivial concern in practice, where long numeric simulations are always fighting the accumulation of computer round-off error. Finally, at equilibrium the relevant eigendirections point along the (potentially) high-dimensional separatrix sur-

face, and so the bifurcation can be mapped through all parameter space. Note that this procedure works no matter the number of dynamical variables involved in the differential equation system. In the next section, we demonstrate how this procedure works for all common normal forms of bifurcations.

III. NORMAL-FORM BIFURCATIONS

Local bifurcations can be described mathematically in a potentially infinite number of ways, but nearly all of them can be reparameterized, at least locally, to one of five kinds of normal forms. These are:

- Saddle-node: $\dot{x} = r + x^2$, where one stable and one unstable fixed point emerge from an previously uninterrupted flow at a critical value r_{crit}
- Transcritical: $\dot{x} = rx - x^2$, where a stable and unstable fixed point always exist, but swap stability at the critical value
- Supercritical Pitchfork: $\dot{x} = rx - x^3$, where symmetric stable fixed points emerge from a single fixed point, which itself becomes unstable
- Subcritical Pitchfork: $\dot{x} = rx + x^3$, symmetric unstable fixed points emerge from an unstable fixed point, which swaps stability

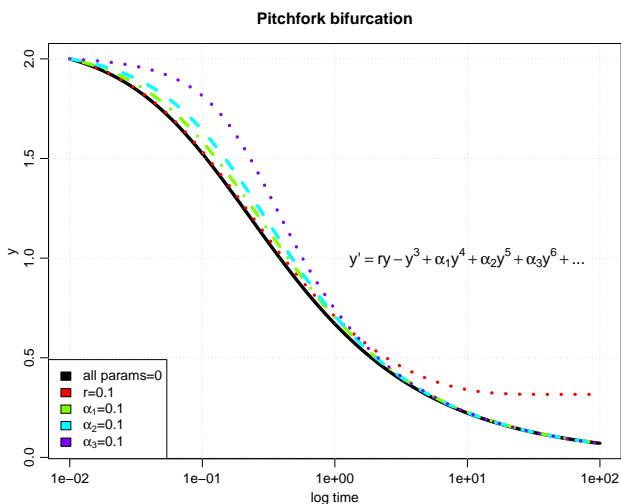


FIG. 2. The trajectory of a supercritical pitchfork at the bifurcation point (black), and slightly perturbed from it (colored lines). At short time scales, high-order parameters (α_3 in this example) appear to be the most significant. But, as the dynamics progress, it becomes clear that r is the only parameter that changes the long-term equilibrium point. This change from important to unimportant (and vice versa) around $t = 5$ is reflected in the arch shape and changing colors of Fig. 3

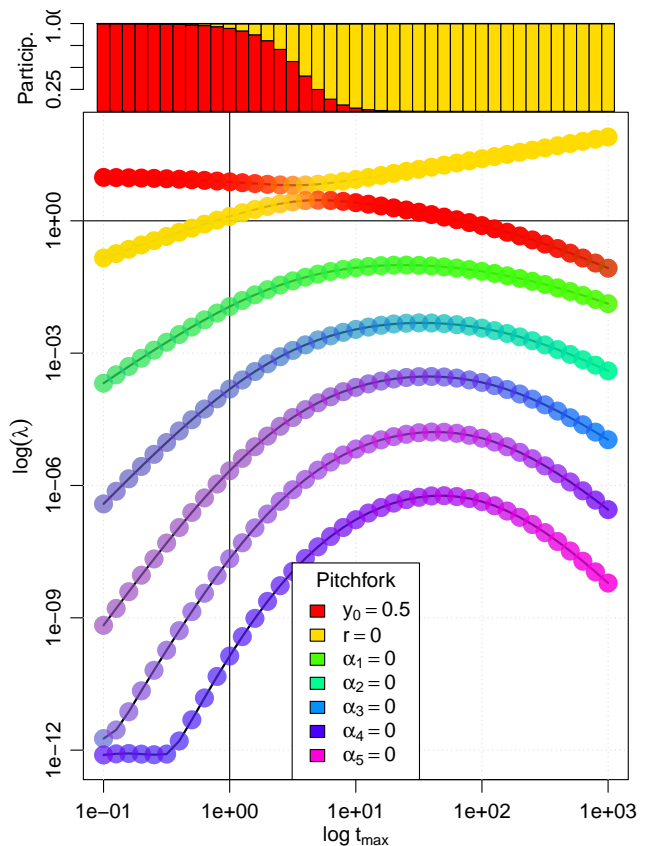


FIG. 3. The eigenvalues of the FIM vs t_{max} , colored by the parameters making up their corresponding eigenvectors. As seen in Fig. 2, the short-term trajectory of a pitchfork bifurcation is driven by many parameters, but the end point by only r . This can be seen in the FIM’s eigenvalues (λ), which initially increase and are dominated by the initial value and the highest order parameter (yellow y_0 and purple α_5). However, as the dynamics run for longer times, red r becomes 100% of the principal eigendirection, while all other parameter combinations lose relevance. With y_0 in the last eigendirection, we can be confident the simulation has run “long enough” for the effect of initial conditions to no longer be unimportant, and equilibrium conditions to have been reached.

- Hopf: a stable limit cycle emerges from what had previously been a stable point attractor. Depending on the coordinate system, the normal form is $\dot{z} = z(a + b|z|^2)$ (complex), $\dot{x} = -y + x(\mu - r^2)$; $\dot{y} = x + y(\mu - r^2)$ (Cartesian), or $\dot{r} = r(\mu - r^2)$; $\dot{\theta} = -1$ (Polar).

A method able to detect bifurcation parameters for these types of bifurcations will detect the overwhelming majority of bifurcations we are likely to encounter.

The Fisher Information as a function of t_{max} for each bifurcation type has a closed-form solution, which complements and validates the numerical results that we present here (see Appendix A). In each case, it becomes clear that in the neighborhood of the bifurcation point, the sensitivity with respect to the bifurcation param-

ter, r , dominates the long-term dynamics of the system, no matter how many other higher order parameters are added to the normal form. For example, a supercritical pitchfork of the form $\dot{y} = ry - y^3 + \alpha_1 y^4 + \alpha_2 y^5 \dots$ experiences a bifurcation when $r = \alpha_i = 0$. At short timescales (e.g., where $t_{max} < 1$), the system's trajectory is strongly influenced by changes to its initial value y_0 and the higher order α terms (for $y_0 > 1$). However, later dynamics show that changes to the α_i 's (and y_0) barely affect the trajectory of approach to equilibrium at 0, while small modifications to r move the equilibrium itself (Fig. 2).

This is reflected in an eigen-analysis of the FIM. Numerical simulations confirm the insight from the analytic solutions and clearly demonstrate the effect of coarse-graining on the system (i.e., increasing t_{max} while keeping the number of samples constant). At very short time scales ($t_{max} < .05$), y_0 is the main participant of the leading eigenvector, and it is then replaced by the largest α_i term; recall from Fig. 2 that this high-order term was equivalently able to bend the trajectory significantly until $t \approx 1$. Around $t = 10$, the change to r begins to have a noticeable influence on the trajectory, and similarly this is the point where r becomes the dominant participant in the leading eigenvector. Note that the leading eigenvalue begins to increase while all others decrease, indicating that the system's bifurcation is co-dimension 1. Note that in this range, small changes to the initial value y_0 have fallen all the way to the last eigenvector, indicating that the system has been allowed to run long enough that transient dynamics have been removed.

Similar figures can be produced for the saddle-node, transcritical, and subcritical pitchfork bifurcation classes. In each case, the eigen-analysis of the FIM indicates

- how long the system should be simulated, by the time it takes for the effect of the initial conditions to reach the least relevant eigenvector
- the co-dimension of the bifurcation (1 in every normal form), by the number of non-decreasing eigenvalues
- the participation factor of each parameter in the hyper/relevant directions by the square of the corresponding eigenvectors (asymptotically approaching 100% r in each case)

These are relatively simple bifurcations, where the separatrix is the hyper-plane $r = 0$. In more complicated situations where the separatrix is a nonlinear combination of bare parameters, this analysis identifies the vector normal to the separatrix. In principle, this local characterization could be extended to map that separatrix (along the hyper/relevant directions) through the high-dimensional parameter space.

Hopf bifurcations present more of a challenge, as they have a fundamentally more complex normal form which does not admit of an easy analytic solution, and a trajectory which can be manipulated in more than one way.

Where the first four bifurcation classes are characterized by the presence and stability of fixed points, Hopf bifurcations are characterized by a limit cycle that emerges from a fixed point, whose radius *and* velocity can be manipulated by model parameters.

Consider the following Hopf bifurcation in Cartesian coordinates, where, as above, additional high order terms have been added:

$$\begin{aligned}\dot{x} &= \beta_1 y + \rho x + \alpha_1 \rho^2 x + \alpha_3 \rho y \\ \dot{y} &= \beta_2 y + \rho y + \alpha_2 \rho^2 y + \alpha_4 \rho x\end{aligned}\quad (5)$$

where $\rho = \mu - (x^2 + y^2)$. In this system, a limit cycle emerges of radius $\sqrt{\mu}$ when $\mu > 0$. As shown in Fig. 4, trajectories beginning near the limit cycle quickly spiral onto it in a counter-clockwise fashion. Adjusting μ slightly (blue) increases the radius of the limit cycle, but the endpoint is at the same angle as the base case and therefore not very distant from the black endpoint. By contrast, increasing the β 's (red) increases the velocity of the cycle, so the red endpoint may well be far from the black endpoint if the dynamic system runs for many cycles. As before, the α_i parameters have only transient effects, and are not shown in Fig. 4 for clarity.

This story can also be well explained using the FIM eigen-analysis applied to the other bifurcation classes above. In Fig. 5, we see up until $t \approx 2\pi$, μ is very slightly more relevant than the β parameters, but after one complete revolution, the trajectory has come very close to the limit cycle whose radius is set by μ , and so changes to μ will not become any more relevant than they already are. By contrast, the velocity of the cycle, set by the β values, continues to increase in relevance as the every sample point in the cycle moves in response to

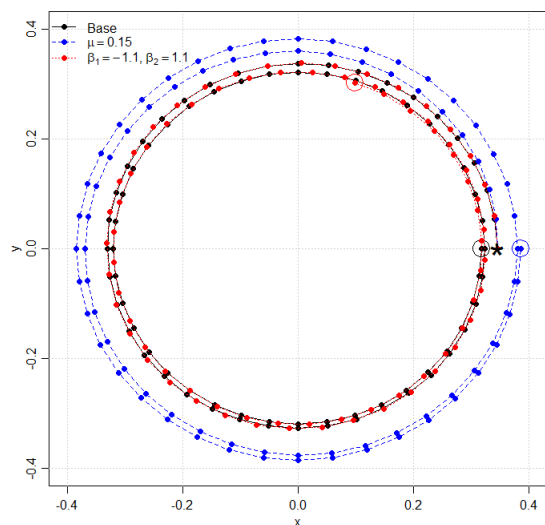


FIG. 4. The Hopf bifurcation, starting with $\mu = 0.1$, $\beta_1 = -1$ and $\beta_2 = 1$, and $y_0 = (.03 + \sqrt{0.1}, 0)$ to start just outside the limit cycle (marked with a *). The trajectory is similar for small changes to μ and the β_i 's, but the resulting endpoints (marked with circles) move much further for β than for μ .

these numbers. The relative importance of β_1 and β_2 is exactly split on both the first and third (not pictured) eigenvectors, while μ takes sole possession of the second eigenvector. Thus, the first eigenvector is hyperrelevant because it controls angular velocity, and the third is relevant because it controls absolute phase. Only the second is relevant due to its involvement in the bifurcation.

IV. BIFURCATIONS IN NON-NORMAL FORMS

Equations describing real systems will often not be written conveniently in one of these normal forms. So even when a researcher knows a system contains a bifurcation, it might not be apparent which one of these it is. For example,

$$mr \frac{\partial^2 \phi}{\partial t^2} = -b \frac{\partial \phi}{\partial t} - mg \sin \phi + mr\omega^2 \sin \phi \cos \phi$$

has a supercritical pitchfork bifurcation, though it might require simulating many values of r and ω to appreciate

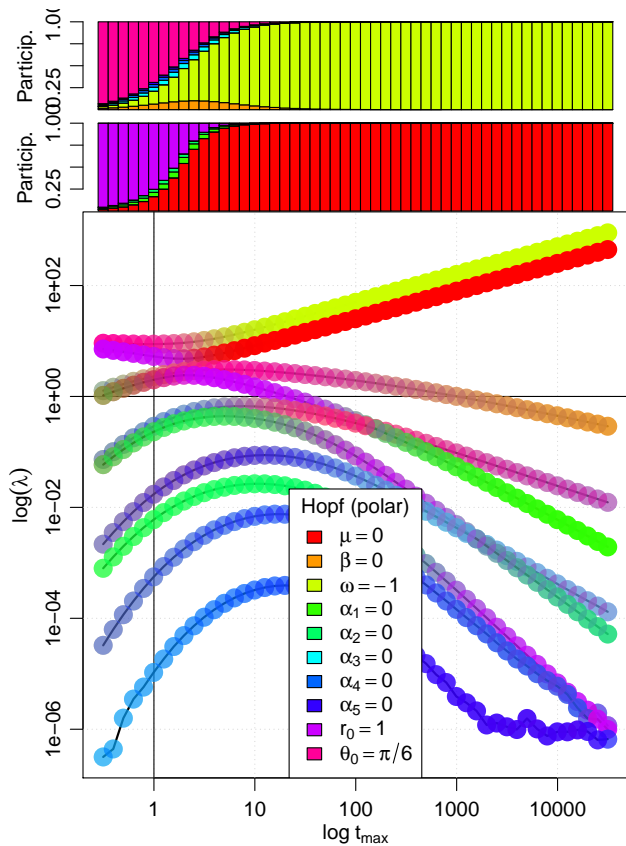


FIG. 5. The eigenvalues of the Hopf bifurcation’s FIM show a dependence on μ that switches from the leading to the second eigenvector after one rotation, and a strong but equal participation both β parameters in the leading and third eigenvector (the β parameters have opposite signs in the first vector, and the same sign in the third.)

this. Similarly, the equation:

$$\dot{y} = r \ln y + y - 1 + \alpha_1(y - 1)^2 + \alpha_2(y - 1)^3 + \dots$$

contains a transcritical bifurcation at $x = 1$ when $r = -1$. However, this only becomes clear after reparameterizing the equation by $R = r + 1$, and $Y = \frac{r}{2}(y - 1)$, when the equation assumes the normal form $\dot{Y} = RY - Y^2 + \mathcal{O}(Y^3)$. Such a substitution might not be immediately apparent to a researcher; however, sloppy model analysis helps clarify the situation.

If the dynamics run for long enough, it becomes clear that only one eigenvalue is relevant while all others fall off, and furthermore the corresponding participation factor becomes dominated exclusively by r (Fig. 6). This tells us that (1) the process has codimension 1, and (2) the reparameterization involves only r . Note that including the initial condition y_0 as a parameter still provides a convenient indication of how long to let the simulation run to be considered “long enough”. That is, if y_0 is participating in the leading eigenvector, this indicates the starting point has a significant effect on the samples, which should ideally not be the case when examining equilibrium behavior. When y_0 begins to drop into the lower eigenvectors, this indicates it is less relevant to the sample data, and the process is therefore well-sampled. It takes somewhat longer for this to occur than in the normal form examples above. Also note that transcritical bifurcations have a leading relevant eigenvalue—rather than a hyperrelevant one—due to a quirk of the normal-form algebra. See Appendix B for a thorough explanation.

But what happens when the situation is not so straightforward? Modifying the above example to the equation $\dot{y} = r \ln(y) + a(y - \alpha) + b(y - \alpha)^2 + \dots$ should still have a transcritical bifurcation for certain parameter values, but no simple reparameterization to create a normal form exists. From above, we can recognize that when a transcritical bifurcation occurs at $y = 1$ for $r = -1, \alpha = 1$. However, when $\alpha \neq 1$, in the neighborhood of $y = \alpha$ all the power terms are zero, but the term $r \ln(y) > 0$ if $\alpha < 1$, suggesting that no fixed point exists in that region. The dis/appearance of a fixed point is the hallmark of a saddle-node bifurcation, and indicates that the allowing a bit of variability in the fixed point’s location has unexpectedly introduced a second codimension to the dynamic system.

This second suggestion is borne out by sloppy analysis, which shows that the equation indeed produces a hyperrelevant eigenvector corresponding to the saddle-node parameter α , which controls the existence—not just the location—of an equilibrium. The transcritical bifurcation still exists, and is controlled by r , as implied by the previous analysis. TWIG allows us to arrive at this conclusion efficiently and unambiguously without a closed-form reparameterization into the normal form.

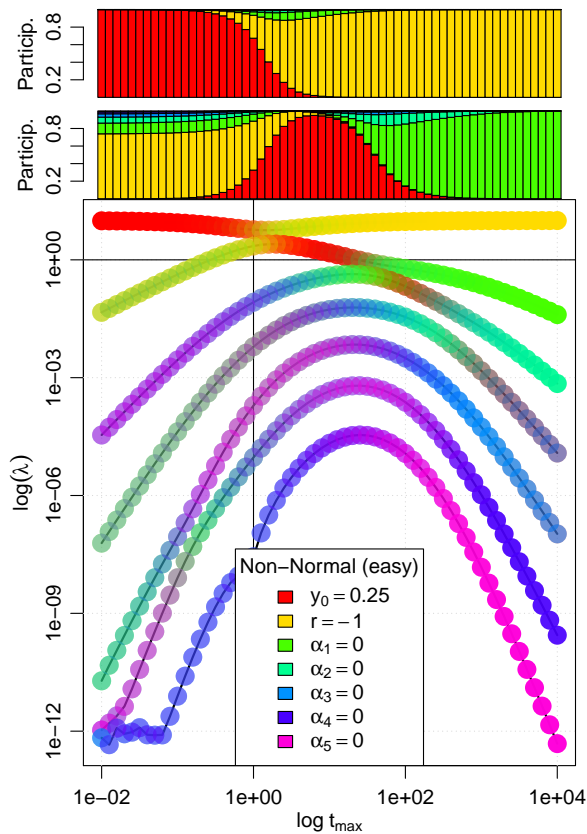


FIG. 6. Equations not in normal form such as $\dot{y} = r \ln y + y - 1 + \alpha_1(y-1)^2 + \alpha_2(y-1)^3 + \dots$ can be interpreted using the same procedure as for normal form bifurcations. As above, the presence of just one non-decreasing eigenvalue, whose corresponding eigenvector is dominated by the single parameter r , indicates that the system has co-dimension 1 and its reparameterization requires only changes to r . The flat leading eigenvalues indicate a transcritical bifurcation.

A. A biophysical example

Glycolysis is a multi-step process which uses the bond energy of glucose to catabolize energy-carrying biomolecules easily usable by cells, and represents one of the dominant processes of all heterotrophic life on earth. A bottleneck in this crucial process is the phosphorylation of fructose-6-phosphate into fructose-1,6-bisphosphate catalyzed by the enzyme phosphofructokinase. The complicated five-species mass-action equation describing this reaction's kinetics can be simplified using Tikhonov's theorem and assuming low concentrations of ATP to the simple dimensionless system:[34, 35]

$$\begin{aligned}\dot{x} &= -x + ay + c_1x^2y + c_2x^3 \\ \dot{y} &= b - ay + c_3x^2y + c_4y^2\end{aligned}$$

where x and y are the concentrations of ADP and F6P respectively, and the four c_i constants are nuisance parameters added to mask the system dynamics. There is

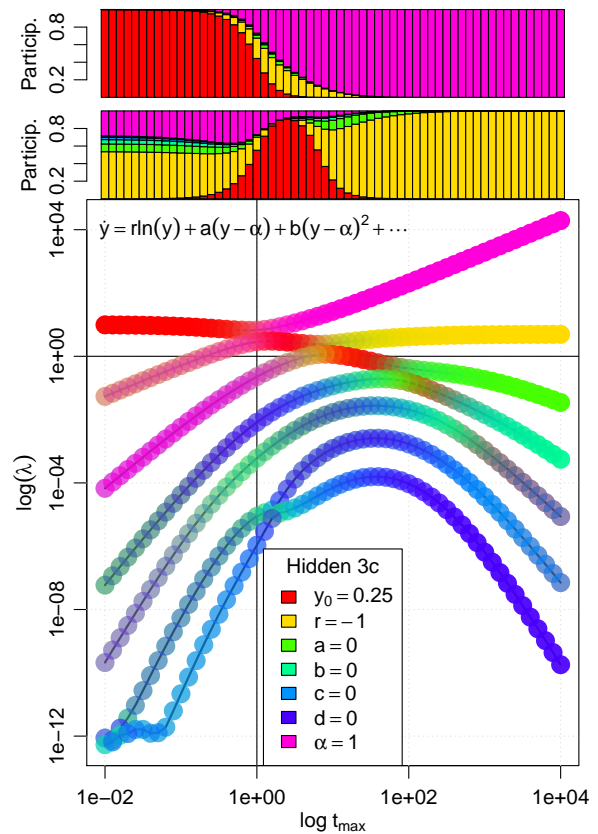


FIG. 7. A difficult non-normal-form transcritical bifurcation can be extremely challenging to analyze analytically, but sloppy analysis indicates one hyperrelevant parameter (corresponding in this case to a saddle-node) and one relevant parameter (usually a clear indicator of a transcritical bifurcation). This means that this system has a bifurcation of codimension 2, and the 1.0 participation factor of in the two directions suggests no recombination of parameters would be required to put the system into a normal form.

a curved bifurcation surface that separates the range of kinetic parameters a, b which lead to either a fixed point at $(b, b/(a+b^2))$ or a stable limit cycle, which can be shown to have the form $b^2 = \frac{1}{2}(1 - 2a \pm \sqrt{1 - 8a})$ [24]. The resulting hypothetical oscillations in glycolytic activity predicted by this analysis have been observed *in vivo* since the early 1970s[36].

A sloppy analysis of this system provides several insights. First, despite the complicated curve described by the separatrix between fixed point and limit cycle in a, b -space, because b can be reparameterized as a function of a it provides only one codimension. Second, the “nuisance” parameter c_4 introduces a change in the period of the oscillations, which means infinitesimal changes in its value cause larger deviations in final trajectory the longer the simulation runs. This shows up as a hyper-relevant direction in TWIG, though it is *not* a second codimension; this is an example of the second caveat mentioned above.

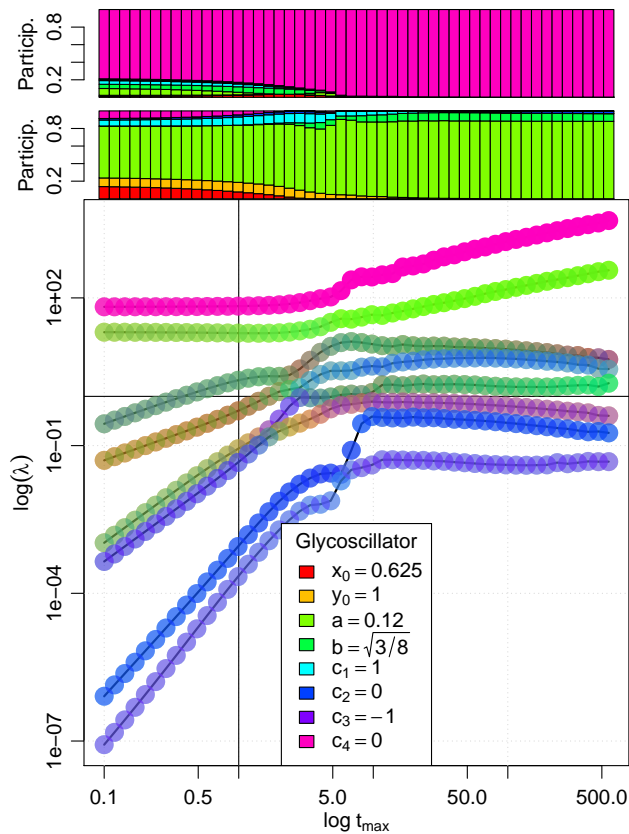


FIG. 8. Analysis of the “glycoscillator” bifurcation. The frequency of the oscillations are driven by c_4 , while the radius of oscillations can be controlled with just one of the a, b parameters discovered by Sel’kov[34].

V. CONCLUSION

Progressive time-dilation of the Fisher Information Matrix as realized by our Time-Widening Information Geometry (TWIG) analysis is an efficient way of characterizing bifurcations in a dynamic system. Researchers have long used eigenanalysis of \mathcal{I} to characterize the “sloppiness” of a system, i.e. its exponential range of sensitivities to parameter changes, and recently leveraged this accumulated expertise with coarse-graining to understand phenomena occurring at distinct time-scales[23, 37]. Building on these insights, we here demonstrate that as t_{max} increases, the changing eigenvalues of \mathcal{I} (and the composition of those eigenvectors) allow us to (1) characterize the co-dimension of the bifurcation, (2) quantify the participation of each bare parameter in the bifurcation, (3) map the bifurcation’s hypersurface (if it is multidimensional), and (4) have an internal check on the length of time necessary to simulate the system to reach equilibrium. These are substantial insights to be gained relatively cheaply, and means that sloppy bifurcation analysis constitutes a powerful tool to supplement traditional analytical analysis,[24, 38] and other specialized analytical tools for high-dimensional

problems[6, 8, 10, 27, 39–41].

Because it is a particularly efficient method of determining important information about high-dimensional bifurcations, we anticipate that TWIG will be particularly important in situations with many components where one or a few bifurcations are expected in each component. These include power grids, circuit boards, interatomic models, complex protein regulatory networks, and ecosystem-based management systems of multiple interacting populations. Such complexity presents substantial difficulties for closed-form analysis, but can be tamed with insights gleaned from this method.

This work was supported by the US National Science Foundation under Award NSF-1753357.

Appendix A: FIM of Saddle-Node Bifurcations

The normal form of the Saddle-node bifurcation is

$$\frac{dy}{dt} = r + y(t)^2 + \alpha_1 y(t)^3 + \alpha_2 y(t)^4 + \dots$$

This differential equation can be solved when all $\theta = 0$ (i.e., at its bifurcation point) by

$$\frac{dy}{dt} = y^2 \rightarrow \frac{dy}{y^2} = dt$$

Integrating both sides yields

$$-\frac{1}{y} \Big|_{y_0}^{y(t)} = t \Big|_0^t \rightarrow \frac{1}{y_0} - \frac{1}{y(t)} = t \rightarrow y(t) = \frac{y_0}{1 - y_0 t}$$

This implies there is a singularity at $t = 1/y_0$, so a proper coarse-graining procedure will involve taking data from $t = 0$ to some value near $1/y_0$, say $0.99/y_0$. As noted in eqn 3, to find the FIM of a system it is only necessary to find the Jacobian, so we need only find the first partial derivative of this data with respect to each parameter in the model.

1. Partial derivative of r

Let the α_i ’s=0. The derivative of the normal form w.r.t. r becomes:

$$\begin{aligned} \frac{\partial}{\partial r} \left(\frac{\partial y}{\partial t} = r + y^2 \right) \\ \frac{\partial^2 y}{\partial r \partial t} = 1 + 2y \frac{\partial y}{\partial r} \end{aligned}$$

We let $w = \frac{\partial y}{\partial r}$, and this becomes $\frac{\partial w}{\partial t} = 1 + 2yw$, which requires the use of an integration factor to solve[42]. If $p_1 y' + p_0 y = q$ then

$$y = \frac{1}{\mu p_1} \left[C + \int \mu q dt \right] \text{ where } \mu = p_1^{-1} \exp \left(\int \frac{p_0}{p_1} dt \right) \quad (\text{A1})$$

Allowing $p_1 = 1$, $p_0 = -2y$, $q = 1$ implies that

$$\begin{aligned}\mu &= 1^{-1} \exp\left(\int \frac{-2y}{1} dt\right) \\ &= \exp\left(-\int \frac{2y_0 dt}{1-y_0 t}\right) \\ &= \exp(2 \ln(1-y_0 t)) \\ &= (1-y_0 t)^2\end{aligned}$$

Therefore,

$$\begin{aligned}w &= \frac{C + \int (1-y_0 t)^2 dt}{(1-y_0 t)^2} \\ &= \frac{C - \frac{(1-y_0 t)^3}{3y_0} \Big|_0^t}{(1-y_0 t)^2} \\ &= \frac{C + \frac{1-(1-y_0 t)^3}{3y_0}}{(1-y_0 t)^2}\end{aligned}$$

Recall this function is being evaluated where the partial derivative $w = \frac{\partial y}{\partial r} = 0$, which implies that $C = -\frac{1-(1-y_0 t)^3}{3y_0}$; when $t = 0$ this further reduces to $C = 0$. Therefore.

$$\frac{\partial y}{\partial r} = \frac{1 - (1 - y_0 t)^3}{3y_0(1 - y_0 t)^2}$$

2. Partial derivative of α_1

Using the same procedure as above,

$$\begin{aligned}\frac{\partial}{\partial \alpha_1} \left(\frac{\partial y}{\partial t} \right) &= \frac{\partial}{\partial \alpha_1} (y^2 + \alpha_1 y^3) \\ \frac{\partial^2 y}{\partial \alpha_1 \partial t} &= 2y \frac{\partial y}{\partial \alpha_1} + y^3 + \cancel{3y^2 \alpha_1} \frac{\partial y}{\partial \alpha_1} \\ \frac{\partial w}{\partial t} &= 2yw + y^3\end{aligned}$$

Note on the second line, we are able to cancel the third term because we are evaluating the slope where α_1 is zero. On the last line, note that p_0 and p_1 are the same as for r , so as above $\mu = (1-y_0 t)^2$, but since now $q = y^3$:

$$\begin{aligned}w &= \frac{C + \int y^3 (1-y_0 t)^2 dt}{(1-y_0 t)^2} \\ &= \frac{C + \int \left(\frac{y_0}{1-y_0 t}\right)^3 (1-y_0 t)^2 dt}{(1-y_0 t)^2} \\ &= \frac{C + \int \frac{y_0^3 dt}{1-y_0 t}}{(1-y_0 t)^2} \\ &= \frac{C - y_0^2 \log(1-y_0 t) \Big|_0^t}{(1-y_0 t)^2} \\ &= \frac{C - y_0^2 \log(1-y_0 t)}{(1-y_0 t)^2}\end{aligned}$$

Again, assuming $w = t = 0 \rightarrow C = 0$, so

$$\frac{\partial y}{\partial \alpha_1} = -\frac{y_0^2 \log(1-y_0 t)}{(1-y_0 t)^2}$$

3. Partial derivatives of higher-order α 's

Higher order terms in the series are of the form $\alpha_n y^{n+2}$ and so

$$\begin{aligned}\frac{\partial}{\partial \alpha_n} \left(\frac{\partial y}{\partial t} = y^2 + \alpha_n y^{n+2} \right) \\ \frac{\partial^2 y}{\partial \alpha_n \partial t} = 2y \frac{\partial y}{\partial \alpha_n} + y^{n+2} + (n+2)y^{n+1} \alpha_n \\ \frac{\partial w}{\partial t} = 2yw + y^{n+2}\end{aligned}$$

We again have the same value of μ , and use integration factors to demonstrate:

$$\begin{aligned}w &= \frac{C + \int \left(\frac{y_0}{1-y_0 t}\right)^{n+2} (1-y_0 t)^2 dt}{(1-y_0 t)^2} \\ &= \frac{C + \int \frac{y_0^{n+2} dt}{(1-y_0 t)^n}}{(1-y_0 t)^2} \\ &= \frac{C - \frac{y_0^{n-1}}{1-n} (1-y_0 t)^{1-n} \Big|_0^t}{(1-y_0 t)^2} \\ &= \frac{C + \frac{y_0^{n-1}}{1-n} (1 - (1-y_0 t)^{1-n})}{(1-y_0 t)^2}\end{aligned}$$

Which again implies that $C = 0$ and so for $n > 1$ we can say

$$\frac{\partial y}{\partial \alpha_n} = \frac{y_0^{n-1} (1 - (1-y_0 t)^{1-n})}{(1-n)(1-y_0 t)^2}$$

Because the Fisher Information Matrix $\mathcal{I} = J^T J$, we can see that element $\mathcal{I}_{1,1}$ will be $\mathcal{O}(y_0^3)$ and all other elements will be higher order. Thus, as y_0 approaches zero, the most important parameter is clearly r .

In the case where \mathcal{I} is being derived from data (or from noise added to a non-/normal form equation), the importance of r can be evaluated by increasing $\sigma^2 \propto y_0^{-3}$. Since, by the central limit theorem standard error $\sigma^2 \propto n$, then the number of time points sampled should decrease as $n \propto y_0^{-3}$.

Appendix B: FIM of Transcritical Bifurcations

These have a similar normal form as the Saddle-node bifurcations above:

$$\frac{dy}{dt} = ry(t) - y(t)^2 + \alpha_1 y(t)^3 + \alpha_2 y(t)^4 + \dots$$

However, the change of sign in the second term causes the differential solution to also have a changed sign:

$$\begin{aligned} \frac{dy}{dt} &= -y^2 \rightarrow -\frac{dy}{y^2} = dt \rightarrow \frac{1}{y} \Big|_{y_0}^{y(t)} = t \Big|_0^t \\ \frac{1}{y(t)} - \frac{1}{y_0} &= t \rightarrow y(t) = \frac{y_0}{1 + y_0 t} \end{aligned}$$

Now the singularity occurs at $t = -\frac{1}{y_0}$, which generally only complicates the coarse-graining if initial conditions are negative.

1. Partial derivative of r

The full solution to the partial derivative of r is somewhat complicated because it depends on y :

$$\begin{aligned} \frac{\partial}{\partial r} \left(\frac{\partial y}{\partial t} = ry - y^2 \right) \\ \frac{\partial^2 y}{\partial r \partial t} &= r \frac{\partial y}{\partial r} + y - 2y \frac{\partial y}{\partial r} \\ \frac{\partial w}{\partial t} &= w(r - 2y) + y \end{aligned}$$

where $w = \frac{\partial y}{\partial r}$. Recall that the derivative is being evaluated where $r = 0$, and so we can argue that

$$\frac{\partial w}{\partial t} + 2yw = y \rightarrow$$

$$\mu = \exp \left(\int \frac{2y_0 dt}{1 + ty_0} \right) = \exp[2 \log(1 + ty_0)] = (1 + ty_0)^2$$

Using our integration factors, we see:

$$\begin{aligned} w &= \frac{C + \int (1 + ty_0)^2 * \frac{y_0}{1 + ty_0} dt}{(1 + ty_0)^2} \\ &= \frac{C + y_0 t (1 + \frac{y_0 t}{2})}{(1 + ty_0)^2} \rightarrow C = 0 \\ &= \frac{y_0 t (2 + y_0 t)}{2(1 + ty_0)^2} = \frac{\partial r}{\partial t} \end{aligned}$$

Note that in the limit that $t \rightarrow \infty$, this expression is order 0 for t ; therefore, unlike other bifurcation classes, transcriticals are expected to have a *relevant*, rather than a hyperrelevant, leading eigenvalue. This was confirmed with simulations (see Fig. 6).

2. Partial derivative of α_1

The derivative can be set up as:

$$\begin{aligned} \frac{\partial}{\partial \alpha_1} \left(\frac{\partial y}{\partial t} = -y^2 + \alpha_1 y^3 \right) \\ \frac{\partial^2 y}{\partial \alpha_1 \partial t} &= -2y \frac{\partial y}{\partial \alpha_1} + 3\alpha_1 y^2 \frac{\partial y}{\partial \alpha_1} + y^3 \\ \frac{\partial w}{\partial t} &= -2yw + y^3 \end{aligned}$$

Since we already know that $\mu = (1 + ty_0)^2$, it follows that

$$\begin{aligned} w &= \frac{C + \int (1 + ty_0)^2 \left(\frac{y_0}{1 + ty_0} \right)^3}{(1 + ty_0)^2} \\ &= \frac{C + y_0^2 \int \frac{y_0}{1 + ty_0}}{(1 + ty_0)^2} \\ &= \frac{C + y_0^2 \log(1 + ty_0)}{(1 + ty_0)^2} \rightarrow C = 0 \\ &= \frac{y_0^2 \log(1 + ty_0)}{(1 + ty_0)^2} \end{aligned}$$

3. Partial derivative of higher-order α 's

Using similar arguments, we arrive at the conclusion that for α_n where $n > 1$

$$\frac{\partial y}{\partial \alpha_n} = \frac{y_0^{n+1} ((1 + ty_0)^{1-n} - 1)}{(1 - n)(1 + ty_0)^2}$$

Plots of the sensitivities suggest that r is the dominant parameter for values of $y_0 < 1$, though exactly where this transition occurs is probably worth investigating.

The first entry in the FIM is $\left(\frac{\partial y}{\partial r} \right)^2$ which is $\mathcal{O}(t^0)$. This implies that the leading eigenvector of transcritical bifurcations will be relevant, not hyperrelevant like for all other forms of bifurcations considered here. It is tempting to speculate that the topological interpretation of this quirk in the algebra stems from the unique flow-field around transcritical bifurcations. For $r < 0$, the vector field has a negative-positive-negative pattern; for $r > 0$ this negative-positive-negative pattern is duplicated, just with an unstable equilibrium at $y = 0$ which had been stable before. Only at the critical value itself ($r = 0$) is there a topological inhomogeneity. The other bifurcations have fundamentally different flow-fields on either side of the critical value, and thus, perhaps, their bifurcation parameters acquire hyper-relevance rather than simply relevance. Further study is needed to prove this conjecture.

Appendix C: FIM of Pitchfork Bifurcations

In the supercritical case, the normal form is

$$\frac{dy}{dt} = ry(t) - y(t)^3 + \alpha_1 y(t)^4 + \alpha_2 y(t)^5 + \dots$$

and the subcritical case is the same except the sign on the cubic term changes. At the critical value of $\theta_i = 0$, the system reduces to:

$$\begin{aligned} \frac{dy}{dt} &= -y^3 \rightarrow -\frac{dy}{y^3} = dt \rightarrow \frac{1}{2y^2} \Big|_{y_0}^{y(t)} = t \Big|_0^t \\ \frac{1}{y(t)^2} - \frac{1}{y_0^2} &= 2t \rightarrow \frac{1}{y(t)^2} = 2t + \frac{1}{y_0^2} \\ &\rightarrow y(t) = \frac{y_0}{\sqrt{1 + 2ty_0^2}} \end{aligned}$$

Following the same logic, the formula for the subcritical case is

$$y(t) = \frac{y_0}{\sqrt{1 - 2ty_0^2}}$$

1. Partial derivative of r

Let the α_i 's=0. The derivative of the normal form w.r.t. r becomes:

$$\begin{aligned} \frac{\partial}{\partial r} \left(\frac{\partial y}{\partial t} = ry - y^3 \right) \\ \frac{\partial^2 y}{\partial r \partial t} = r \frac{\partial y}{\partial r} + y - 3y^2 \frac{\partial y}{\partial r} \\ \frac{\partial w}{\partial t} = y - 3y^2 w \end{aligned}$$

where $w = \frac{\partial y}{\partial r}$. Using integration factors $p_1 = 1, p_0 = 3y^2, q = y$, we see that

$$\begin{aligned} \mu &= \exp \left(\int -3y^2 dt \right) \\ &= \exp \left(- \int \frac{3y_0^2 dt}{1 + 2y_0^2 t} \right) \\ &= \exp \left(\frac{3}{2} \ln(1 + 2y_0^2 t) \right) \\ &= (1 + 2y_0^2 t)^{3/2} \end{aligned}$$

Therefore,

$$\begin{aligned} w &= \frac{C + \int \mu y(t) dt}{\mu} \\ &= \frac{\mathcal{C} + \int \frac{y_0}{\sqrt{1+2ty_0^2}} (1 + 2y_0^2 t)^{3/2} dt}{(1 + 2y_0^2 t)^{3/2}} \\ \frac{\partial y}{\partial r} &= \frac{y_0 t (1 + y_0^2 t)}{(1 + 2y_0^2 t)^{3/2}} \end{aligned}$$

Following the same logic for the subcritical case eventually brings us to ...

2. Partial derivative of α 's

When $r = 0$, and all $\alpha_{i \neq n} = 0$, then the normal form reduces to

$$\frac{dy}{dt} = -y(t)^3 + \alpha_n y(t)^{n+3}$$

which conveniently allows us to use the same μ integration factor as above. Using the integration scheme outlined there, after many steps we reach the conclusion that

$$\frac{d\alpha_n}{dt} = \frac{y_0^{n+1} (1 + 2ty_0^2)^{1-n/2} - 1}{2 - n} \mu$$

This produces an obvious problem when $n = 2$, but in that case the integration step simplifies and we find that

$$\frac{d\alpha_2}{dt} = \frac{y_0^3 \ln(1 + 2ty_0^2)}{2\mu}$$

All this indicates that in the FIM, the entry corresponding to $(\partial y / \partial r)^2$ is $\mathcal{O}(t^1)$, while all other entries are lower order, so r will be the only hyperrelevant direction.

Appendix D: FIM of Hopf Bifurcations

Analysis of the Hopf bifurcation in either the complex or Cartesian formulation is complicated, because the introduction of nuisance parameters to the normal form equations tends to alter the period of limit cycles. This means standard trigonometric functions would also need to be altered with time-dependent terms to dilate/expand the period for a closed form solution of the trajectories $z(t)$ or $x(t), y(t)$ respectively.

However, reparameterizing the equation into polar coordinate form simplifies matters greatly. The system $\dot{r} = r(\mu - r^2); \dot{\theta} = -1$ should look familiar, as the equation for r is simply the normal form for a supercritical pitchfork bifurcation. Therefore, deriving the elements of its Fisher Information Matrix have already been performed above, albeit with different variable and parameter names.

-
- [1] P. Hartman, *Ordinary Differential Equations* (SIAM, Philadelphia, 1982) p. 632.
- [2] Quote from p. 1021 of J. D. Crawford, Introduction to bifurcation theory, *Reviews of Modern Physics* **63**, 991 (1991).
- [3] Simple Neural Networks that Optimize Decisions, *International Journal of Bifurcation and Chaos* **15**, 803 (2005).
- [4] S. Feng, P. Holmes, A. Rorie, and W. T. Newsome, Can Monkeys Choose Optimally When Faced with Noisy Stimuli and Unequal Rewards?, *PLOS Computational Biology* **5**, e1000284 (2009).
- [5] I. M. Sobol, Sensitivity Estimates for Nonlinear Mathematical Models, *Mathematical Modeling in Civil Engineering* **1**, 407 (1993).
- [6] B. Bettonvil and J. P. Kleijnen, Searching for important factors in simulation models with many factors: Sequential bifurcation, *European Journal of Operational Research* **96**, 180 (1997).
- [7] T. Homma and A. Saltelli, Importance measures in global sensitivity analysis of nonlinear models, *Reliability Engineering and System Safety* **52**, 1 (1996).
- [8] R. Gul and S. Bernhard, Parametric uncertainty and

- global sensitivity analysis in a model of the carotid bifurcation: Identification and ranking of most sensitive model parameters, *Mathematical Biosciences* **269**, 104 (2015).
- [9] A. Berezhkovskii and A. Szabo, One-dimensional reaction coordinates for diffusive activated rate processes in many dimensions, *Journal of Chemical Physics* **122**, 10.1063/1.1818091 (2005).
- [10] M. J. Feigenbaum, Quantitative Universality for a Class of Nonlinear Transformations, *Journal of Statistical Physics* **19**, 25 (1978).
- [11] M. J. Feigenbaum, The universal metric properties of nonlinear transformations, *Journal of Statistical Physics* **21**, 669 (1979).
- [12] M. Widom and L. P. Kadanoff, Renormalization group analysis of bifurcations in area-preserving maps, *Physica D: Nonlinear Phenomena* **5**, 287 (1982).
- [13] B. Hu and J. Rudnick, Exact solutions to the feigenbaum renormalization-group equations for intermittency, *Physical Review Letters* **48**, 1645 (1982).
- [14] J. Hu, *Renormalization, rigidity, and universality in bifurcation theory*, Ph.D. thesis, City University of New York, New York (1995).
- [15] D. Hathcock and J. P. Sethna, Reaction rates and the noisy saddle-node bifurcation: Renormalization group for barrier crossing, *Physical Review Research* **3**, 10.1103/PhysRevResearch.3.013156 (2021).
- [16] L.-N. Chang and N.-P. Chang, Bifurcation and Dynamical Symmetry Breaking in a Renormalization-Group-Improved Field Theory, *Physical Review Letters* **54**, 2407 (1985).
- [17] R. E. DeVille, A. Harkin, M. Holzer, K. Josić, and T. J. Kaper, Analysis of a renormalization group method and normal form theory for perturbed ordinary differential equations, *Physica D: Nonlinear Phenomena* **237**, 1029 (2008).
- [18] M. K. Transtrum, B. B. Machta, K. S. Brown, B. C. Daniels, C. R. Myers, and J. P. Sethna, Perspective: Slowness and emergent theories in physics, biology, and beyond, *The Journal of Chemical Physics* **143**, 010901 (2015).
- [19] M. K. Transtrum, B. B. Machta, and J. P. Sethna, Why are nonlinear fits to data so challenging?, *Physical Review Letters* **104**, 2 (2010).
- [20] M. K. Transtrum and P. Qiu, Bridging Mechanistic and Phenomenological Models of Complex Biological Systems (2016), arXiv:1509.06278v2.
- [21] B. B. Machta, R. Chachra, M. Transtrum, and J. P. Sethna, Parameter Space Compression Underlies Emergent Theories and Predictive Models, *Science* **342**, 604 (2013), arXiv:1303.6738v1.
- [22] K. S. Brown, C. C. Hill, G. A. Calero, C. R. Myers, K. H. Lee, J. P. Sethna, and R. A. Cerione, The statistical mechanics of complex signaling networks: Nerve growth factor signaling, *Physical Biology* **1**, 184 (2004), arXiv:0406043 [q-bio].
- [23] A. Raju, B. B. Machta, and J. P. Sethna, Information loss under coarse graining: A geometric approach, *Physical Review E* **98**, 052112 (2018).
- [24] Figure 7.3.7 in S. H. Strogatz, *Nonlinear dynamics and chaos: With applications to physics, biology, chemistry, and engineering*, 2nd ed. (Westview Press, Boulder, CO, 2015) p. 513.
- [25] O. Jiménez-Ramírez, E. J. Cruz-Domínguez, M. A. Quiroz-Juárez, J. L. Aragón, and R. Vázquez-Medina, Experimental detection of Hopf bifurcation in two-dimensional dynamical systems, *Chaos, Solitons & Fractals: X* **6**, 100058 (2021).
- [26] J. P. C. Kleijnen, B. Bettonvil, and F. Persson, Screening for the Important Factors in Large Discrete-Event Simulation Models: Sequential Bifurcation and Its Applications, *Screening: Methods for Experimentation in Industry, Drug Discovery, and Genetics*, 287 (2006).
- [27] S. Waldherr and F. Allgower, A feedback approach to bifurcation analysis in biochemical networks with many parameters, *Proceedings of the FOSBE 2007*, 479 (2007), arXiv:0711.2687.
- [28] M. K. Transtrum, B. B. Machta, and J. P. Sethna, Geometry of nonlinear least squares with applications to sloppy models and optimization, *Physical Review E* **83**, 36701 (2011).
- [29] A. F. Brouwer and M. C. Eisenberg, The underlying connections between identifiability, active subspaces, and parameter space dimension reduction, arXiv:1802.05641 (2018).
- [30] I. Bendixson, Sur les courbes définies par des équations différentielles, *Acta Mathematica* **24**, 1 (1901).
- [31] B. L. Francis and M. K. Transtrum, Unwinding the model manifold: Choosing similarity measures to remove local minima in sloppy dynamical systems, *Physical Review E* **100**, 14 (2019).
- [32] I. J. Pérez-Arriaga, G. C. Verghese, and F. C. Schweppe, Selective modal analysis with applications to electric power systems, part i: Heuristic introduction, *IEEE Transactions on Power Apparatus and Systems* **PAS-101**, 3117 (1982).
- [33] F. Garofalo, L. Iannelli, and F. Vasca, Participation factors and their connections to residues and relative gain array, *IFAC Proceedings Volumes* **35**, 125 (2002).
- [34] Self-Oscillations in Glycolysis I. A Simple Kinetic Model, *European Journal of Biochemistry* **4**, 79 (1968).
- [35] A. N. Tikhonov, On the dependence of the solutions of differential equations on a small parameter, *Matematicheskii Sbornik. Novaya Seriya* **22**, 193 (1948).
- [36] B. Chance, G. Williamson, I. Lee, L. Mela, D. DeVault, A. Ghosh, and E. Pye, Synchronization Phenomena in Oscillations of Yeast Cells and Isolated Mitochondria, in *Biological and Biochemical Oscillators* (Academic Press, 1973) pp. 285–300.
- [37] R. Chachra, M. K. Transtrum, and J. P. Sethna, Structural susceptibility and separation of time scales in the van der Pol oscillator, *Physical Review E* **86**, 026712 (2012).
- [38] S. N. Rasband, *Chaotic Dynamics of Nonlinear Systems*, 2nd ed. (Wiley, New York, NY, 1990) p. 230.
- [39] D. A. Rand, A. Raju, M. Saez, F. Corson, and E. D. Siggia, *Geometry of Gene Regulatory Dynamics* (2021), arXiv:2105.13722.
- [40] J. Guckenheimer and P. Holmes, *Nonlinear Oscillations Dynamical Systems, and Bifurcations of Vector Fields* (Springer New York, 1983) p. 497.
- [41] P. D. Kirk, T. Toni, and M. P. Stumpf, Parameter inference for biochemical systems that undergo a Hopf bifurcation, *Biophysical Journal* **95**, 540 (2008).
- [42] See equation 14.2.1 in S. Hassani, *Mathematical Physics: A Modern Introduction to Its Foundations*, 2nd ed. (Springer, Heidelberg, 2013) p. 1205.